Shape Evolution by Surface Diffusion and Surface Attachment Limited Kinetics on Completely Faceted Surfaces

by

W. C. Carter, A. R. Roosen and J. W. Cahn
Materials Science and Engineering Laboratory
NIST, Gaithersburg, MD 20899
and
J. E. Taylor
Mathematics Dept., Rutgers University
New Brunswick, New Jersey

ABSTRACT

The evolution of two-dimensional shapes to equilibrium shapes is investigated for two kinetic mechanisms, surface diffusion and surface attachment limited kinetics. Qualitative differences are found that may be used in experiments for easy distinction among the two mechanisms, and find topological changes not expected for the corresponding isotropic problems. We take advantage of the mathematical developments for surface evolution and equilibration problems when surface energy anisotropy is "crystalline," so extreme that crystals are fully faceted. We confirm the prediction that with this anisotropy these problems are more easily solvable than for lesser anisotropies, and the techniques developed may even be useful for approximating isotropic problems.

1 Introduction

Modeling interface growth and shape changes is fundamental to the study of microstructural evolution, but tracking of the evolution of an interface during diffusive transport is a notoriously difficult problem, especially for anisotropic surface energies. Use of the *crystalline* formulation, in which the interfaces are assumed to be completely faceted, can avoid many of these difficulties. In this paper, we apply this crystalline formulation to the special cases of sintering, coarsening, and shape equilibration where the only driving force comes from the reduction of the energy associated with surfaces and where volume is conserved. No other thermodynamic driving forces, such as those which accompany phase changes, are assumed present here, and flows which do not conserve volume, such as motion by mean curvature (e.g. grain growth) are treated elsewhere. (See [1] for a review.)

Volume conserving surface motion typically arises with heterophase surfaces in which long range diffusion of a conserved quantity is required for motion. We will assume that surface velocities are entirely determined by surface processes; either the diffusion is confined to be along the surface (SD) or with more general diffusion in a surrounding transport medium that the motion is limited by surface attachment limited kinetics (SALK). To have volume conservation we have to assume no change in the amount of matter stored in the transport medium. With these restrictions we obtain geometric laws for surface motion, which allow us to apply recently developed methods for calculating the time evolution of shapes. Part of these developments is the realization that although these laws become very difficult with mild surface energy anisotropies, they become simpler if the anisotropy in surface energy is so extreme that all microstructures are composed of plane segments of a finite number of low energy orientations, for some problems even simpler than the isotropic cases. We therefore explore in this paper this extreme case of anisotropy. Last we restrict ourselves to evolution of shapes on the plane, two-dimensional polygonal "particles."

The surface energy function, $\gamma(\mathbf{n})$, which underlies the driving force, is the work at constant pressure and temperature which must be supplied to create a unit area (length in two-dimensions) of surface with orientation $\mathbf{n}$. It is useful to represent $\gamma(\mathbf{n})$ by the shape with the lowest surface energy for a fixed volume, the Wulff shape $\mathcal{W}_\gamma$. For the special case that $\gamma(\mathbf{n})$ is a constant, $\mathcal{W}_\gamma$ is a sphere (circle in two dimensions). When $\gamma(\mathbf{n})$ is not constant, the shape $\mathcal{W}_\gamma$ differs from a sphere and in extreme cases becomes polyhedral. For a general $\gamma(\mathbf{n})$ in any dimension, $\mathcal{W}_\gamma$ is given by the Wulff construction: $\mathcal{W}_\gamma = \{\mathbf{x} : \mathbf{x}\cdot\mathbf{n} \leq \gamma(\mathbf{n}) \text{ for all } \mathbf{n}\}$. Note that in this construction the length scales of $\mathcal{W}_\gamma$ have units of γ. The distance that a facet is from the origin of $\mathcal{W}_\gamma$ is $\gamma(\mathbf{n})$ for that $\mathbf{n}$, but the length Λ of that facet in $\mathcal{W}_\gamma$ depends not only on the γ of that facet but also those of the two adjacent facets. The Wulff construction can be easily inverted to recover $\gamma(\mathbf{n})$ for those $\mathbf{n}$ that appear in $\mathcal{W}_\gamma$. If $\mathcal{W}_\gamma$ has missing orientations, the values of γ for those $\mathbf{n}$ not in $\mathcal{W}_\gamma$ cannot in general be recovered, but usually do not appear in physical problems.

Recently developed methods [2, 3] have shown that computations of surface evolution can often be greatly simplified when $\mathcal{W}_\gamma$ is "crystalline", that is completely faceted (composed of only flat surfaces and their intersections). In this case, the underlying surface energy density $\gamma(\mathbf{n})$ can be given as a list of magnitudes for all orientations $\mathbf{n}$ which are the normal of a facet in $\mathcal{W}_\gamma$. Any orientations not in $\mathcal{W}_\gamma$ will break up into facets that do appear in $\mathcal{W}_\gamma$ while preserving the average orientation of the surface.

We are interested in motions which decrease surface energy. The limit of change in surface energy with volume under small deformations is by definition the *weighted mean curvature* (or *weighted curvature* in two dimensions), κ^γ [4].[1] "Small" usually means local, but in the case of facets should mean motion of an entire facet by a small distance. κ^γ is thus defined on a facet-by-facet basis by considering energy changes involved in moving the entire facet keeping its normal direction fixed. While the chemical potential may vary along a facet, the average chemical potential across the facet equals κ^γ on that facet. For polygonal $\mathcal{W}_\gamma$, κ^γ has a particularly simple form, based on $\mathcal{W}_\gamma$, given in Section 2.

The methods developed for anisotropic problems can be useful for approximating isotropic problems. Motion by crystalline curvature, where the normal velocity of each facet e is proportional to its crystalline curvature and volume is not conserved, has been proven to converge to motion by (isotropic) curvature for two dimensional problems, as $\mathcal{W}_\gamma$ approaches a circle (though a sequence of regular polygons with the number of sides becoming infinite) [5, 6, 7]. It remains to be shown whether other types of motion will likewise converge to the isotropic case. In the case of surface diffusion, there does not now exist a good way of computing isotropic surface diffusion, so its approximation by this crystalline method is currently the best way of computing it, assuming that these approximations do in fact converge to it.

2 2D Formulation

In this section we reexamine in the crystalline formulation two limiting cases of geometric interface motion that conserve volume. The first arises from surface diffusion (SD); with isotropic surfaces, this is motion

[1] We have picked a sign convention throughout for κ^γ in which a convex body (such as a sphere with the "solid" region being inside, or any Wulff shape) has positive κ^γ. This sign convention is opposite to that in [4] and in differential geometry, where the mean curvature vector points in the direction in which the surface curves and which is thus a negative multiple of the unit normal vector for a convex body, but it is in accordance to the way the isotropic Gibbs-Thomsen equation is typically written: $\mu = \mu_o + V_o\gamma\kappa$.

by the Laplacian of mean curvature. The second arises from surface attachment limited kinetics (SALK) with fast transport through a surrounding surface layer or medium assumed; with isotropic surfaces and linear kinetics, this is motion by mean curvature modified for volume conservation to become motion by the difference between curvature and a suitably weighted average of mean curvature.

2.1 Basic definitions

Let γ be a surface energy density function such that the Wulff shape $\mathcal{W}_\gamma$ is a polygon having M edges, called *facets* in this paper, of lengths $\Lambda_0, \Lambda_1, \ldots, \Lambda_{M-1}$ as $\mathcal{W}_\gamma$ is traversed in a positive (counter-clockwise) direction. The directions of the unit normals $\mathbf{n}_i$, common to both the surface at time t, $S(t)$, and $\mathcal{W}_\gamma$, are defined as pointing away from the region which we will denote as "solid." (We will use the terminology "surface" in spite of the fact that we are dealing with 1-dimensional polygonal curves.) Initial data is given as the set, $A(0)$, which is the area covered by the crystal. The surface $S(0)$ is a collection of non-intersecting polygons which are the boundary of $A(0)$ such that each "facet" (edge) e_i is parallel to some facet of $\mathcal{W}_\gamma$, and that if e_i and e_j are consecutive facets in $S(0)$, they have normal directions that are adjacent, consecutive in either direction, in $\mathcal{W}_\gamma$. We shall see that this "adjacency" condition is preserved. $S(0)$ is oriented so that the "solid" region is to the left as the interface is traversed in the positive direction. Note that some of the polygons may be completely contained within other polygons (indicating the existence of 'holes' in the solid), and the surface may be quite complicated, having a very large number of facets some of which have zero length. We will focus on one of these polygons, a simply closed surface with N facets with positive finite lengths $\{L_0, L_1, \ldots, L_{N-1}\}$.

In the usual case, motion of each facet is parallel to itself, with velocity v_i, that is positive if it is in the direction of $\mathbf{n}_i$. Sometimes, a single facet will break into two or more facets by the insertion of one or more *steps* (short facets of neighboring orientations). $S(t)$ will always be polygonal, but the number of facets may change due to disappearance of facets or insertion of steps according to rules that we will discuss in Section 3.

The weighted curvature $\kappa^{\gamma}{}_i$ of facet e_i is inversely proportional to L_i [4]:

$$\kappa^{\gamma}{}_i = \sigma_i \Lambda(\mathbf{n}_i)/L_i \tag{1}$$

where σ_i is a "convexity" factor that is $+1$, 0, or -1 depending on how e_i abuts its neighbors: Fig. 1. If both ends of e_i are *regular*, i.e. the corner is a left turn proceeding around the surface counter-clockwise, then $\sigma_i = +1$ since the change in energy by moving e_i in the direction of $\mathbf{n}_i$ is positive. If both are *inverse* (both right turns), then $\sigma_i = -1$. If one is regular and the other inverse, then $\sigma_i = 0$; because of the adjacency condition, the energy gained at one end by the motion of e_i is exactly compensated by a loss at the other end. Note that the surface energy factor in this equation is $\Lambda(\mathbf{n}_i)$ instead of $\gamma(\mathbf{n}_i)$ because the change in surface energy with volume due to motion of the facet is

$$\frac{\gamma(\mathbf{n}_{i+1}) - \mathbf{n}_i \cdot \mathbf{n}_{i+1}\gamma(\mathbf{n}_i)}{\sqrt{1-(\mathbf{n}_i \cdot \mathbf{n}_{i+1})^2}} + \frac{\gamma(\mathbf{n}_{i-1}) - \mathbf{n}_i \cdot \mathbf{n}_{i-1}\gamma(\mathbf{n}_i)}{\sqrt{1-(\mathbf{n}_i \cdot \mathbf{n}_{i-1})^2}} \tag{2}$$

which also happens to be the formula to compute $\Lambda(\mathbf{n}_i)$.)

2.2 Surface Diffusion: Motion by $\nabla_s^2\mu$

In surface diffusion, mass flux is confined to the surface and is is driven by gradients in chemical potential $\mu(s,t)$ that vary with position s along a surface. In this section, we discuss the case where a facet moves without the creation of any new facets; conditions for stepping are discussed in section 3.

The surface recedes at places where there is a positive divergence of flux (a negative accumulation) and advances where the divergence is negative. Volume (area in two-dimensions) inside a surface is conserved. When a facet remains flat, the velocity at any given time t must be constant along it:

$$v_i(t) = -\nabla_s \cdot J_i(s,t) = constant(t) \tag{3}$$

Here, $v_i(t)$ has been scaled by a constant, a_o, related to the atomic size of the diffusing species in the solid; the actual velocity is $a_o v_i$. Here s is the position along e_i: $0 \le s < L_i$. All gradients are restricted to the interface–in this case they derivatives with respect to arc length.

The flux $J_i(s,t)$ along e_i is given by Ficks first law:

$$J_i(s,t) = -D_i \nabla_s \mu_i(s,t) \tag{4}$$

where D_i is the surface diffusion coefficient for the i^{th} facet.

When a facet moves a distance dx the free energy change is associated with addition of new length at the two ends: the change of surface energy of the polygon is $\kappa^{\gamma}{}_i L_i dx$, where is $\kappa^{\gamma}{}_i$ is the weighted curvature (weighted mean curvature in 3D). In all such problems there is an arbitrary 0 for μ, which we will take as the chemical potential of a crystal with infinitely large facets. With this choice for the 0 for μ, the energy change of incorporating the atoms into the solid is $dx \cdot \int_0^{L_i} \mu_i(s)ds$. For equilibrium with respect to facet motion,

$$\kappa^{\gamma}{}_i L_i = \int_0^{L_i} \mu_i(s)ds = \sigma_i \Lambda_i \tag{5}$$

Thus the average chemical potential equals κ^γ on e_i:

$$\kappa^\gamma{}_i = \frac{\int_0^{L_i} \mu_i(s)ds}{L_i} \tag{6}$$

Equations 4, 3 and 6 together are the crystalline formulation of motion by the Laplacian of mean curvature when the surfaces are isotropic.

Integration of Equations 4 and 3 give that for each facet the chemical potential is parabolic in s:

$$\mu_i(s,t) = \mu_i - \frac{J_i}{D_i}s + \frac{v_i}{2D_i}s^2 \tag{7}$$

where the $2N$ integration constants $\mu_i \equiv \mu_i(0)$ and $J_i \equiv J_i(0)$ are the chemical potential and flux at the corner, $s = 0$ of each facet, and the N values of v_i are to be determined. Since the surface is closed, e_N is e_0; hence

$$J_N = J_0; \quad \mu_N = \mu_0. \tag{8}$$

Continuity of chemical potential and flux at the corners gives $2N$ equations

$$\mu_{i+1} = \mu_i - \frac{J_i}{D_i}L_i + \frac{v_i}{2D_i}{L_i}^2 \tag{9}$$

$$J_{i+1} = J_i - v_i L_i \tag{10}$$

Furthermore, Equation 10 and 8 imply that

$$0 = \sum_{i=0}^{N-1} v_i L_i \tag{11}$$

so, the enclosed area is conserved as it should be for surface diffusion. Equations 8, 9, and 10, and imply:

$$0 = \sum_{i=0}^{N-1} \frac{L_i}{D_i}(J_i + J_{i+1}) \tag{12}$$

Equations 6 and 7 give N more equations:

$$v_i = \frac{6D_i(\kappa^\gamma{}_i - \mu_i) + 3J_iL_i}{{L_i}^2} \tag{13}$$

Equations 9, 10, and 13 form $3N$ equations in $3N$ unknowns and completely determine the flow, v_i, for each closed surface in terms of all the L.

The lengths, L_i, of the facets can be transformed into distances, d_i, from a fixed origin with:

$$L_i = \pm \frac{d_{i+1} - \mathbf{n}_i \cdot \mathbf{n}_{i+1} d_i}{\sqrt{1 - (\mathbf{n}_i \cdot \mathbf{n}_{i+1})^2}} \pm \frac{d_{i-1} - \mathbf{n}_i \cdot \mathbf{n}_{i-1} d_i}{\sqrt{1 - (\mathbf{n}_i \cdot \mathbf{n}_{i-1})^2}}, \tag{14}$$

in which each term is $+$ if the corner is regular, and $-$ if not. From this follows a system of ordinary differential equations for the lengths in terms of the velocities:

$$\frac{dL_i}{dt} = \pm \frac{v_{i+1} - \mathbf{n}_i \cdot \mathbf{n}_{i+1} v_i}{\sqrt{1 - (\mathbf{n}_i \cdot \mathbf{n}_{i+1})^2}} \pm \frac{v_{i-1} - \mathbf{n}_i \cdot \mathbf{n}_{i-1} v_i}{\sqrt{1 - (\mathbf{n}_i \cdot \mathbf{n}_{i-1})^2}}. \tag{15}$$

2.3 Surface Attachment Limited Kinetics: Motion by $\kappa^\gamma$with a volume constraint

Motion by $\overline{\kappa^\gamma} - \kappa^\gamma$ (where $\overline{\kappa^\gamma}$ is the average of κ^γ) is another limiting case of volume conserving flow. The solid is assumed to be surrounded by a low density and/or low volume phase, possibly a thin surface layer, in which diffusion is so fast that the chemical potential is kept homogeneous at all times, and in which the total mass of the components of the solid is assumed so small that changes in its mass can be neglected. If the surrounding "phase" is an adsorbed layer this is a special case of surface diffusion with the surface diffusivity large compared to the attachment rate. With surface diffusion the flux is limited to each connected surface, and the volume each encloses is conserved. If the surrounding phase is a vapor or solvent phase, the evaporation/condensation or the dissolution/precipitation kinetics are assumed slow and linear in the supersaturation modified for κ^γ. For this problem the surface of the solid need not be single closed curve; the solid can be many particles, and with modification there even can be disconnected pores. Volume conservation holds for the sum of volumes of surfaces bounding each connected region of the surrounding phase.

Matter is exchanged between the solid and the surrounding transport medium at a rate that is locally uniform for each facet. The rate at which new material accumulates along a facet e_i is taken to be proportional to the difference between the current value of the chemical potential in the vapor (or any solvent) phase and the average chemical potential along the surface. The velocity of the surface is $v = \rho m a_o(\Omega - \mu)$ where Ω is the chemical potential in the ambient phase and μ is the local value of the chemical potential at the surface; ρ is the density of attachment sites and m is the attachment rate [2] at the defect sites. We make the assumption that attachment sites are spatially uncorrelated, so that the suitably averaged ρ can be sensibly defined for each type of facet at scales which are implicit in the crystalline model.

[2] We will not make a distinction between the kinetic law of attachment or detachment. The velocity is assumed to be an odd function of $\Omega - \mu$.

On the average, each facet remains flat and the averaged velocity is:

$$v_i \ = M_i(\Omega - \kappa^{\gamma}{}_i) \tag{16}$$

where M_i is the averaged mobility on e_i and is related to averages of ρ, a_o, and m_i.

Since area is conserved, $\sum_{i=0}^{N-1} v_i L_i = 0$, Ω is found to be a mobility and length average of κ^{γ}:

$$\Omega = \frac{\sum_{i=0}^{N-1} M_i L_i \kappa^{\gamma}{}_i}{\sum_{i=0}^{N-1} M_i L_i} \tag{17}$$

Note that the velocities go to zero as a surface shape approaches the Wulff shape, or as the weighted mean curvature approaches a constant for each of the connected surfaces. An average is taken as above for each set of interfaces which can exchange mass which will depend on the physical problem which is being modeled. For instance, during coarsening of a collection of particles, averages would be taken over all the exterior surfaces of particles but the interiors (pores) would be averaged separately. Each time a topological change occurs in the system, the set of surfaces which would be averaged together may gain or lose members.

3 Production and Disappearance of Facets

It is possible that in the course of motion, some facets will become of zero length. It is also possible that for reasons of stability new facets ought to be created either in the initial surface and/or in the course of motion. These issues are addressed in this section.

Facets with $\sigma = 0$ are qualitatively different from facets with $\sigma \neq 0$. If a facet with $\sigma \neq 0$ approaches zero length, its chemical potential becomes infinite; this happens only when an entire particle is shrinking to a point, and thus never happens when volume is conserved for each particle (as is always true for SD and sometimes taken to be true for SALK). On the other hand, if a facet of weighted mean curvature zero is reduced to zero length, then its potential converges to 0 and the facet can simply be removed; its adjacent facets become collinear and are simply merged to one segment. This entire process of replace three segments by one is called *merging.*

Adding new facets is the reverse of this process. Facets of nonzero σ can be introduced only where the potential is already infinite (as, for example, in an initial surface with corners that are too sharp, omitting directions that are directions in $\mathcal{W}_{\gamma}$). But a facet of zero length and zero weighted mean curvature can be inserted in a pre-existing facet at a place where the potential is zero, dividing that pre-existing facet into two facets. There are two senses in which such a facet could be inserted; the conditions under which one should make such insertions and which sense to use is discussed under the appropriate rule (SD or SALK) below. The production of new facets by inserting $\sigma = 0$ facets has been called *shattering* by Roosen[2] and refers to the production of many facets during motion of crystalline interfaces in a diffusion field. Here, since the production of many facets turns out not to happen, we use the word *stepping* to refer to the process of replacing one facet by two collinear facets (the sum of whose lengths is that of the original facet) connected by a zero-length facet of zero weighted mean curvature.

3.1 Surface Diffusion

3.1.1 Elimination of facets

Let e_s be a facet which is shrinking toward zero length due to its motion and the motion of the neighboring facets. There are two cases to consider: $\sigma_s \neq 0$ and $\sigma_s = 0$.

We claim that a facet with $\sigma_s \neq 0$ never approaches zero length, since if it did, equations 1 and 6 would imply that μ becomes unbounded on e_s with the same sign as σ_s as $L_s \to 0$. If the neighboring facets are not also all having their potentials becoming unbounded at the same rate (and with the same sign) then that would also produce infinite gradients in potential and provide an infinite driving force to lengthen the edge. And because there is volume conservation, it is not possible for all edges in connected component to go to zero length simultaneously. (Proofs will appear in [8].)

If $\sigma_s = 0$, then as the length $L_s \to 0$, $\mu \to 0$ along e_s since ${\kappa^\gamma}_s = 0$. If the change in flux across the facet is also going to zero, then the facet can disappear "in place" as its neighbors become collinear; in this case we merge the neighbors, as stated above. Otherwise if the change in flux is larger than $\mathcal{O}(L_s)$, by equation 10 its velocity will become very large. The small facet will either: rapidly move to a position, if it exists, where the flux entering e_s matches the exiting flux; or, if such a position does not exist, it will move rapidly until one of its adjacent segments also becomes very short, with most of its length having been effectively transferred to the other adjacent segment, Fig. 2. In the second case, as this adjacent segment becomes short, with nonzero change of flux across it, it too begins to move rapidly (see Eq. 10). That makes the original short segment rapidly become longer, and as it grows longer it rapidly slows its motion, squeezing the new short facet very much but not down to zero length. The new short facet in its rapid motion again effectively transfers the length of the neighbor ahead of it back onto the neighbor behind it (the one that used to be short), until the neighbor ahead of the moving facet itself becomes short (See Figure 2). This process of successive short, increasingly rapidly moving facets continues until the fluxes across the short facets match; often this occurs when there is another rapidly moving short facet coming from the opposite direction and several facets annihilate at the same instant. The motion of the short facets occurs on a time-scale which is rapid compared to the rest of the polygon: a facet becomes short at one position, the short step zigs along the curve, apparently around its corners, disappearing somewhere far away. Since the larger facets are nearly stationary during this short period of time, the interface looks much like it did before the small facets settled or annihilated but with differently named segments occupying the positions of the original segments.

3.2 Stepping

Physically, it seems possible that different parts of an edge could move at different speeds. Since a moving edge is actually composed of atomic ledges, the situation could arise that many ledges gather in one place, effectively splitting an edge in two on a large scale. Because all edges must retain fixed normal directions, we refer to this process as *stepping* in which a single edge splits into two edges having the same normal direction connected by a small edge having a different normal. Below, we rigourously define a *stepping*, and define conditions under which such steps would be introduced.

A *stepping* as a point at which a vanishingly small facet e_s is introduced in the middle of a facet e_B to produce three facets e_{s-1}, e_s, and e_{s+1} such that $e_{s\pm1}$ have the same normal direction as the initial edge. This zero-length facet e_s will have $\sigma_s = 0$ and $L_s = 0$, while $L_{s-1} + L_{s+1} = L_B$. $\sigma_{s\pm1}$ will be determined by the *sense* of the stepping (i.e. whether the direction of e_s precedes or follows the direction of e_B in the Wulff shape), and the types of corners at the ends of e_B (i.e. whether the corners are regular or inverse). We are interested in computing motions that are stable, in the sense that small perturbations of the surface at some time should not result in differences that grow in time. In our crystalline model, perturbations are accomplished by steppings, and we need to ensure that any stepping that will grow will be made.

We say that a particular configuration of zero and non-zero-length edges at time t has its associated potential (defined according to the equations of Section 2) *stable* if no zero-length facet has infinite velocity, if all zero-length facets become of positive length for some immediately subsequent interval of time (t, T) when motion is given by the equations of Section 2, and if no additional zero-length edges can be inserted while maintaining these conditions. This last statement is not one that is easy to check, however. We give below criteria which are easy to check, and which imply the statements above if it is true (as we believe) that there is a unique collection of steppings and resulting potential which is stable for any initial polygon with no zero-length edges.

We distinguish two types of stepping events for motions which are governed at all times by stable potentials: those events which take place at *topological times* (including the initial time $t = 0$) where the structure of the interfaces changes in some topological way and thereby those that take place at *regular times* where one or more facets find it advantageous to step in to several pieces. An algorithm for finding a stepping which results in a stable potential at topological times is described in section 4.

At both types of times, in order for the velocity of a zero-length edge e_s to be finite, Equation 6 implies that $\mu_s = 0 = \mu_{s+1}$ and Equation 10 implies that $J_s = J_{s+1}$ (since v_s is of order $(J_{s+1} - J_s)/L_s$). Also, at both types of times, the zero-length edge is required to grow in time. If such a stable point exists, then it is also required that the facet grow in order for e_s to appear.

At a regular time T, there is a potential μ which is the limit of the potentials as time comes up to T. We assert that the potential should be continuous at T – that the potentials computed after inserting a zero-length step should be the same as that inherited from μ. Thus a stepping should be considered at any point where the potential μ is zero, and where a sense can be chosen so that the velocities computed for the resulting neighbors e_{s+1} and e_{s-1} (using the appropriate values for their average potentials) are the same as that of the unstepped edge. Alternatively, this condition could be considered as the neighboring edges having the correct average potentials when they are assumed to have the potential as that inherited from the unstepped edge. This continuity of potential over regular times follows from the assumption of stability at previous times: if a step can be inserted at a point where $\mu = 0$ and where the velocities of the neighbors become different and related to each other in such a way that the step will grow, then such a step would also have been favorable at some previous time, and not inserting it then would violate the hypothesis of the surface and its potential being stable at all times.

Thus the criterion for stepping is:

Approach I From the current μ, create steps on facet e_B at the zeros of μ, and for each sense for the steps, determine if the averages of μ_B on the resulting facets have the correct values given by their weighted mean curvatures. For example, if there is one zero of μ and it occurs at cL_B, then check whether

$$\kappa^{\gamma}{}_{s-1} = \frac{\int_0^{cL_B} \mu_B(x)dx}{cL_B}, \qquad \kappa^{\gamma}{}_{s+1} = \frac{\int_{cL_B}^{L_B} \mu_B(x)dx}{(1-c)L_B} \tag{18}$$

If this is true, then check whether the length of the inserted segments will grow in time, and if so, make that stepping. On the other hand, if $\sigma_{s-1} \neq 0$ and

$$\sigma_{s-1} \int_0^{cL_B} \mu_B(x)dx > \Lambda(\mathbf{n}_{s-1}) \tag{19}$$

then a stepping there would have facets e_{s-1} and e_{s+1} being driven apart with an initially positive rather than zero velocity, and so one must be at a topological time. In this case, the potential μ cannot be continuously converted into a stable potential, and an entirely new potential must be computed. If $\sigma_{s-1} \neq 0$ and

$$\sigma_{s-1} \int_0^{cL_B} \mu_B(x)dx < \Lambda(\mathbf{n}_{s-1}) \tag{20}$$

then facets e_{s-1} and e_{s+1} would be driven back together and that stepping should not be made. Equivalent (and consistent) statements hold in the case that $\sigma_{s+1} \neq 0$. In case $\sigma_B = 0$ and the sense of the stepping is such that $\sigma_{s-1} = 0 = \sigma_{s+1}$, then such a stepping can only be good if $c = 0$ or 1 (and then only if it will grow in time, an additional condition to check as always).

Approach II An equivalent and clearer approach is to use the Cahn-Hoffman ξ vector formulation. ξ should have the properties that for each corner (e_{B-1}, e_B) of the surface, the value of ξ is the vector which is the corner of the Wulff shape $\mathcal{W}_\gamma$ corresponding to the orientations $\mathbf{n}_{B-1}$ and $\mathbf{n}_B$, and so that $\nabla_s \cdot \xi = \mu$ along each facet. Because the potential μ computed according to Section 2 has the property that $\int_{e_B} \mu = \sigma_B \Lambda(\mathbf{n}_B)$, where $\Lambda(\mathbf{n}_B)$ is the length of the facet in $\mathcal{W}_\gamma$ with normal $\mathbf{n}_B$, the ξ so computed is single-valued and continuous. We see that ξ is thus uniquely determined by the surface (including any zero-length edges) and its associated μ. In particular, note that the value of ξ at the two endpoints of a $\sigma = 0$ facet is the same. Critical points of ξ will always occur at the zeroes of μ, since μ is the derivative of ξ. If this ξ has the property that except on corners of the surface ξ is always within the interior of a facet of $\mathcal{W}_\gamma$, then in particular any critical point of the ξ is, and this implies that the potential μ is stable. The value of ξ at a zero of μ being in the interior of a facet of $\mathcal{W}_\gamma$ means that the velocities of the segments computed by making a stepping at the zero and the correct averages for the potentials would be different from each other and would be such as to drive the two segments back together). If ξ ever extends beyond the ends of the appropriate facet, then the μ is definitely not stable; this is a case where the velocities computed from the correct averages of the potentials would drive the two facets apart with positive velocity and mean that a topological change has just occurred (since otherwise the previously computed potentials could not have been stable). Such bad-ξ potentials are in fact an indication that steppings must be made at those topological times and the potential recomputed. If a critical point occurs at value of ξ which is on a corner of $\mathcal{W}_\gamma$, one should consider a stepping at that point, and again, the stepping should be kept only if the zero-length segment becomes of nonzero length as time progresses. The ξ vector is particularly easy to visualize, since its dependence of position along a facet is cubic (being the integral of the quadratic potential).

Motion by surface diffusion should also be gradient flow in the H^{-1} inner product [9]. Given functions

u,v with $\int u = \int v = 0$, their H^{-1} inner product $u \bullet v$ is $-\int u\phi_v$, where ϕ_v is the inverse Laplacian of v – that is, ϕ_v satisfies $\nabla_s^2 \phi_v = v$. In our case, v is a set of velocities $\{v_i\}$ for facets, and $\int v = 0$ is the condition $\sum v_i L_i = 0$; ϕ_v is the potential μ, computed so that the continuity conditions hold. (Such a potential is determined only up to a constant a, but the constant does not matter for the minimization since $\sum u_i a L_i = 0$.) If v is motion by gradient flow in this inner product, it should minimize $\int v\kappa^\gamma + \frac{1}{2} v \bullet v$ [10]. For the case of crystalline curves being considered in this paper, this means that over all possible velocities and steps we should minimize

$$\frac{1}{2} v \bullet v + \sum_i \sigma_i \Lambda_i v_i. \tag{21}$$

If $\{v_i\}$ minimizes this quantity, and if we use δ_k to mean velocity is 1 on segment k and 0 on other segments, then for each k,

$$\begin{aligned}
\sigma_k \Lambda_k &= \frac{\partial}{\partial v_k}(-\frac{1}{2} v \bullet v) \\
&= -v \bullet \delta_v \\
&= \int \phi_v \delta_v \\
&= \int_0^{L_k} (\mu_k - J_k/D_k s + v_k s^2/2D_k)\, ds \\
&= L_k \mu_k - J_k L_k^2/2D_k + v_k L_k^3/6D_k
\end{aligned} \tag{22}$$

This reduces to the previous condition 13:

$$\kappa^\gamma{}_k = \mu_k - J_k L_k/2D_k + v_k L_k^2/6D_k. \tag{23}$$

On the other hand, if by introducing additional zero-length steps and recomputing μ we can reduce 21 further, we should do it. In particular, introducing further steps when one has a potential which is not stable does so reduce the above sum. The optimal stepping has been achieved if and only if the sum cannot be further reduced. To show that this H^{-1} gradient flow approach is the same as the previous two, it would be sufficient to prove that there is a unique stable potential for the boundary of any given region bounded by a crystalline curve.

3.3 Surface Attachment-Limited Kinetics (SALK)

3.3.1 Facet elimination

Just as in surface diffusion, facets with zero weighted mean curvature may be eliminated by having one neighbor overtake another. If a facet with non-zero weighted mean curvature shrinks to zero length, then all segments on its connected component must also be shrinking to zero length. (As $L_s \rightarrow 0$, $\sigma_s \kappa^{\gamma}{}_s \rightarrow \infty$, and unless the average Ω also becomes infinite, v_s will be so as to lengthen rather than shrink the facet.) This cannot happen if the average Ω is made separately for each connected component of the surface (the case of a thin vapor layer), so in this case a facet with σ_s nonzero will never shrink to zero length. But for coarsening, where there is instantaneous long-range diffusion through the vapor, it can certainly happen that small grains shrink while larger ones grow.

3.3.2 Stepping

We show that stepping is never favored for SALK at regular (non-topological) times.

There are two cases to consider: stepping a facet with $\sigma \neq 0$ and stepping one with $\sigma = 0$.

Consider stepping e_B with $\sigma \neq 0$. Three new facets are produced: one zero length facet with $\sigma = 0$ and its two neighbors. One neighbor must have its $\sigma = 0$ and the other will have a $\sigma = \sigma_B$. Equation 16 implies that the difference in velocities is $v_{s+1} - v_{s-1} = -\kappa^{\gamma}{}_{s+1}$, where e_{s+1} has been taken to have the nonzero σ. If $\sigma > 0$ that difference is negative, so e_s disappears; the same holds for $\sigma < 0$.

Consider stepping e_B with $\sigma = 0$. After the stepping, either $\sigma_{s+1} = -\sigma_{s-1} \neq 0$ or $\sigma_{s+1} = \sigma_{s-1} = 0$. (The step has the sense that the new neighbors have σ with opposite sign, or they both have $\sigma = 0$). If $\sigma_{s+1} > \sigma_{s-1}$, then $v_{s+1} - v_{s-1}$ is necessarily negative and stepping is not favorable, and similarly for $\sigma_{s+1} < \sigma_{s-1}$ (Figure 1). However, if the both new neighbors have $\sigma = 0$, then all three will move with the same velocity. The small facet e_s is neutrally stable; if it was inserted, it will travel to one of the nearby corners at with constant speed where it will subsequently annihilate. The inserted facet does not lengthen, and thus it not inserted.

3.4 Topological Changes

When different parts of a surface collide, a topological change must be made. For simplicity, we make the assumption that if $\mathbf{n}$ is a normal to $\mathcal{W}_\gamma$, then so is $-\mathbf{n}$. The collision is thus between oppositely oriented segments (since segments bound solids and/or “outside” regions); as a limiting case, two corners may collide, in which case either pair of oppositely oriented normals could be used. If one facet completely overlaps the opposite, the shorter facet is completely removed, as is the section of the longer facet that overlaps the shorter. Then the remaining portions of the longer facet are connected to the neighbors of the shorter one. If the opposing facets only partially overlap, then the portion of overlap is removed from both facets, and the remaining piece is attached to the loose former neighbor of the other facet.

This cutting and pasting will produce bad corners, i.e. ones which omit normals of the Wulff shape (unless $\mathcal{W}_\gamma$ is a parallelogram). These illegal corners will have infinite chemical potential and are places where zero-length $\sigma \neq 0$ facets must be inserted until none of the normals of $\mathcal{W}_\gamma$ between neighboring edges are omitted. These new edges will move with initially infinite velocity, although the velocity will immediately become finite as the edges become of non-zero length. it remains to be shown that there is indeed an unique evolution in SD or in SALK out of such a corner.

In SALK it is possible for an entire connected component to shrink to a point if there is more than one component surrounded by the same transport medium. If this occurs, all its edges are simultaneously removed. The total average curvature, which is the chemical potential in the transport medium, drops by an amount equal to the length of the boundary of $\mathcal{W}_\gamma$ (or some weighted sum of the Λ_i if the M_i are not all equal to 1).

4 Numerical computations

4.1 General Purpose Data Structures

General purpose data structures for the motion of completely faceted, two-dimensional surfaces as described in [2] were used. To adapt that program to this problem involved changing the formula by which the velocity of a facet is computed. These crystalline methods work for initial data consistent with definitions in section 2.1 and can automatically handle topological changes in the surface.

4.2 Surface Diffusion

Two parts of the computation are described below. In Section 4.2.1, we describe the means by which we calculate a chemical potential along the surface given a particular configuration of edges. In Section 4.2.2 we describe how steps are introduced at each time step as necessary to assure that the chemical potential is stable.

4.2.1 Calculating Potentials

A hybrid of two numerical schemes is used.

The first scheme relies on the observation that because the recursion relations 9 and 10 are linear, the values of the flux and potential at any facet is a linear function of the the values at the first facet:

$$J_i = A_{J_i} + B_{J_i} J_0 + C_{J_i} \mu_0 \tag{24}$$
$$\mu_i = A_{\mu_i} + B_{\mu_i} J_0 + C_{\mu_i} \mu_0.$$

Here each of the A_{X_i}, B_{X_i}, and C_{X_i} are complicated functions of $(\kappa^\gamma{}_0, \ldots, \kappa^\gamma{}_{i-1}; D_0, \ldots, D_{i-1}; L_0, \ldots, L_{i-1})$ which can be numerically computed for a particular configuration of facets using 9 and 10 by the following stratagem: Let μ_0 and J_0 be unknowns, but calculate from the recursion relations 9 and 10, μ_N and J_N for the case that $\mu_0 = 0$ and $J_0 = 0$; $A_{J_N} = J_N$ and $A_{\mu_N} = \mu_N$. The B_{X_N} can be calculated by setting $J_0 = 1$ and $\mu_0 = 0$ and the C_{X_N} are calculated similarly. Because the final endpoint of segment N is the initial point of segment 1, $\mu_N = \mu_0$ and $J_N = J_0$ (equation 8, the unknowns J_0 and μ_0 can be determined directly from the solution of the two linear equations 24. All J_i, μ_i, and v_i can then be determined by recursion equations 9- 13.

While this method lends itself to rapid computation, it is numerically unstable when there is even a mildly disparate range of facet lengths. Truncation errors currently render it useless for more than around 20 facets. The problem is alleviated by using structures which can manipulate numbers with arbitrary precision, but the computations rapidly become slower as the number of facets in a surface increases and the necessary precision increases. Because of the lack of speed, this method is only used when the following scheme becomes unreliable.

The second method of solution is a conjugate gradient scheme[11] which is typically an N^2 iterative scheme. To implement the conjugate gradient, the recursion equations can be written as a linear system:

$$\left(\begin{array}{ccc|ccc} & \alpha_{mm} & & & \alpha_{mJ} & \\ & & & & & \\ --- & --- & --- & --- & --- & --- \\ & & & & & \\ & \alpha_{Jm} & & & \alpha_{JJ} & \end{array}\right) \begin{bmatrix} \mu_0 \\ \mu_1 \\ \vdots \\ \mu_{N-1} \\ -- \\ J_0 \\ J_1 \\ \vdots \\ J_{N-1} \end{bmatrix} = 6 \begin{bmatrix} \kappa^\gamma{}_0 \\ \kappa^\gamma{}_1 \\ \vdots \\ \kappa^\gamma{}_{N-1} \\ -- \\ \kappa^\gamma{}_0 \\ \kappa^\gamma{}_1 \\ \vdots \\ \kappa^\gamma{}_{N-1} \end{bmatrix} \tag{25}$$

where,

$$\alpha_{mm} = \begin{pmatrix} 4 & 2 & 0 & 0 & \dots & 0 \\ 0 & 4 & 2 & 0 & & \vdots \\ 0 & 0 & 4 & 2 & \ddots & \\ \vdots & & & \ddots & \ddots & 0 \\ 0 & & & & & 2 \\ 2 & 0 & \dots & & 0 & 4 \end{pmatrix} \qquad \alpha_{mJ} = \begin{pmatrix} \frac{-L_0}{D_0} & 0 & \dots & & 0 \\ 0 & \frac{-L_1}{D_1} & \ddots & & \vdots \\ \vdots & \ddots & \ddots & & \\ & & & & \\ \vdots & & & & 0 \\ 0 & \dots & & 0 & \frac{-L_{N-1}}{D_{N-1}} \end{pmatrix} \tag{26}$$

$$\alpha_{Jm} = \begin{pmatrix} 6 & 0 & \dots & & 0 \\ 0 & 6 & \ddots & & \vdots \\ \vdots & \ddots & \ddots & & \\ \vdots & & & & 0 \\ 0 & \dots & & 0 & 6 \end{pmatrix} \qquad \alpha_{JJ} = \begin{pmatrix} \frac{-2L_0}{D_0} & \frac{-L_0}{D_0} & 0 & \dots & 0 \\ 0 & \frac{-2L_1}{D_1} & \frac{-L_1}{D_1} & & \vdots \\ 0 & 0 & \frac{-2L_2}{D_2} & \ddots & 0 \\ 0 & & & & \frac{-L_{N-2}}{D_{N-2}} \\ \frac{-L_{N-1}}{D_{N-1}} & 0 & \dots & 0 & \frac{-2L_{N-1}}{D_{N-1}} \end{pmatrix} \tag{27}$$

Conjugate gradient iteration works by squaring the difference of equation 25 and iterating the positive definite system by choosing an optimal set of iteration directions. Squaring the system also squares the condition number of the matrix, which makes the numerical precision worse for small condition numbers. Experience has shown that the stability of the conjugate gradient methods is increasingly worse as the length scales of a particular surface become more disparate, and when this occurs the first scheme is applied using arbitrary precision numbers.

Integration in time is performed explicitly with time steps being chosen dynamically so that no pair of edges may overrun an intervening edge and so that no edge velocity may change too rapidly.

4.2.2 Stepping Algorithm

Because the time steps are of non-zero size, it will never be the case that an facet may be introduced precisely when it first becomes stable, but in fact the system will be in an unstable state. Thus the algorithm for calculating stepping is the same both at "topological" times and at "regular" times.

The algorithm to perform the stepping is based upon the fact that the ξ vector must always remain within certain bounds for each facet (Section 3.2). Assuming the above computation has been performed to compute the starting chemical potential μ_{start} along each facet for a particular configuration of facets, it is easy to compute for each facet whether the condition on the ξ vector holds. If not, then that edge must be stepped. There are always one or two zero's of μ_{start} along such an edge, and steps are introduced at those zeros for which the ξ vector exceeds its bounds. The sense of the introduced step is taken in the opposite direction from the flux across the step: if μ_{start} is decreasing from right to left across the step, then the step will have the next normal direction in $\mathcal{W}_\gamma$ from the original facet counting counterclockwise around $\mathcal{W}_\gamma$.

Once all edges have been checked for ξ, and all steps have been introduced, the chemical potential is recomputed using the first method above, but keeping $\mu = 0$ at each of the new steps and allowing the flux to be discontinuous across the step. A discontinuous flux across a zero-length step implies that it should move at infinite velocity, and so each such step is moved so as to iteratively find the point at which the flux is continuous across the step. Finally, each of the non-step edges is moved according to the finally calculated chemical potential, which will expand each of the steps so that they will not be of zero length.

4.2.3 Surface Attachment Limited Kinetics

With Equations 16 and 17, calculation of the velocities is immediate and the same scheme of forward differencing the system of ODEs, Eq. 15, applies. Results are illustrated below.

5 Example Computations

The time evolution for 5 different sets of initial data, including comparisons between surface diffusion (SD) and surface attachment limited kinetics (SALK) are illustrated in Figures 3-7. Computations of SD are displayed in a time sequence of light gray images, while images for SALK are in dark gray. The kinetic coefficients in each case have been scaled so that evolution occurs roughly on the same time scale for each.

In Figure 3, $\mathcal{W}_\gamma$ is a square. The initial data is an elongated rectangle. Figure 4 begins with the same initial data, but uses a 16-gon as its Wulff shape. Note that in both cases, the particle flowing by SALK remains convex. In contrast, particle flowing by SD becomes non-convex, forming “bulbs” on the ends of the initial rectangle. These examples show an important difference between SD and SALK. In SD, motion is so as to reduce local gradients in chemical potential, and this “proximity effect” can produce non-convex regions from previously convex ones. In SALK, by contrast, convex regions always will remain convex because there is no local force driving them to become concave.

In Figure 5 the analog of the rectangle has been rotated by $\pi/8$. $\mathcal{W}_\gamma$ is a square, and so what was a rectangle is now a pair of staircases. Here, not only is the flow different for SALK and SD, but the end configuration as well. For SALK, volume diffuses uniformly to the zero κ^γ stairsteps from the positive κ^γ ends causing all the steps not adjacent to the ends to move diagonally as a unit, since equations 16 and 17 imply that all facets with $\kappa^\gamma = 0$ move with the same velocity. In motion by SD, on the other hand, the middle region of the zero κ^γ steps hardly moves at all. The steps near the end are removed one by one as volume is pumped from the ends towards the center. In fact, the small edges are rapidly moving off down the staircase as described in Section 3.1.1. Eventually, the particle breaks into two particles each of which asymptotically approach $\mathcal{W}_\gamma$. The ability to detect and handle such topological changes is one of the strengths of the general computational scheme. This example further demonstrates how SALK cannot take non-convex curves to convex ones. The staircase in Figure 5 is the crystalline analog to a convex curve in the surface energy sense: it contains no points of negative curvature.

One might wonder if it is possible that stepping might only occur at "topological times", as it does in Figures 3 and 4, in which all stepping occurs only at the start of the computation. Figure 6 shows that this is not the case, and that stepping may occur in SD even at regular times. The Wulff shape is again a square, and the initial condition is L-shaped, having one of the branches very elongated. In SD flow, bulbs form on the ends of each branch at time $t = 0$ via the proximity effect. Interestingly, another step forms on the inside long edge of the L so as to turn the single long edge into a long zero κ^γ edge and an edge with negative curvature at the base of the shorter leg of the L. The two legs of the L shrink at approximately the same speed, and so the shorter leg becomes a single bulb before the bulb at the other end of the long leg has time to travel down the leg. Note that as the short leg shrinks, the edge which initially formed the outside of the short leg becomes very short, and runs up the long leg, eventually disappearing. At even later times, the material that was contained in the short leg eventually reforms itself into a large bulb and then motion continues as for the elongated rectangle. It is important to note, however, that a new step formed as the blob on the short leg turned the corner to begin moving down the long leg.

Topological changes may occur in a surprising and complicated manner. The spiral in Figure 7 is an illustrative example for a square $\mathcal{W}_\gamma$. Initially the ends of the spiral have large positive κ^γ, and the 'interior' facets have zero or small κ^γ. Most of the action takes place at the inner end where $\kappa^\gamma$and the gradient in μ is very large. As the inner end unwraps and forms bulbs (a manifestation of the proximity effect), it collides with another part of the crystal forming a hole. The two surfaces then flow independently, until they collide again, re-forming a simply connected domain. The process repeats once: the system approaches an equilibrium $\mathcal{W}_\gamma$ with a Wulff-shaped hole in it. Note that the flow does not scale uniformly with log($time$). Each of the topological changes produces large discontinuous changes in the chemical potential which reestablish large potential gradients in regions which had previously nearly exhausted them. Thus, the overall effect is that the evolution starts fast and slows until a topological change occurs, and then proceeds rapidly in those regions proximate to the event which caused the topological change.

Although the spiral of Figure 7 did not undergo a topological change under SALK, it is possible to have initial data which does produce topological changes for that type of flow. Figure 8, which uses an octagonal Wulff shape, starts as a large particle with a deep notch cut out of it. Under both flow by SALK and by SD, the notch closes off and the system equilibrates to a Wulff-shaped crystal with a Wulff-shaped hole in it. The reason the flow by SALK is able to produce the topological change is because of the two opposing zero-κ^γfacets. Because the initial shape is a simply connected solid, the average $\kappa^\gamma$is positive. Thus all zero curvature facets have the same positive velocity, and so they can be placed so as to collide.

6 Discussion

In this paper we have set up a problem of shape evolution, driven entirely by reduction in an interfacial energy that is so anisotropic that only shapes with a limited set of facets orientations need be considered. This is called crystalline anisotropy. In this extreme of anisotropy, problems of equilibrium and shape evolution become much simpler than with lesser anisotropy, and in many cases simpler even than with isotropy. This paper is an exploration the crystalline formulations for this type of problem specialized to 2-D. Three dimensional problems are generally more difficult, but there are many reasons to believe that the advantages of the crystalline formulation will be even greater.

We considered two kinds of material flows, surface diffusion (SD) and surface attachment limited kinetics (SALK). For SD we postulated a chemical potential field in a surrounding transport medium that varies continuously with position along the surface and around corners. Fluxes, proportional to gradients in chemical potential, are required to be continuous at corners, and to have a constant divergence on each facet proportional to the instantaneous growth rate of that facet. Furthermore the chemical potential at each facet is required to have an average value so that there is no free energy change when the facet moves to grow or dissolve the crystal—an averaged local equilibrium. For SALK we assumed that the kinetic process of attachment or detachment is so slow compared to diffusion in the transport medium, that the chemical potential in that medium is constant, and that the interface motion of each facet was a function, here taken to be linear, of the local deviation from equilibrium. The surrounding transport medium could be the surface as in surface diffusion or, with special restrictions, a surrounding vapor or solution phase.

An immediate advantage of the crystalline formulation is that we are able to show that solutions exist for all times for SD and SALK. At present only short time solutions have been shown to exist for the isotropic SD problem.

We have set up an algorithm for solving the evolution equations and solved them for specific anisotropies as parameterized by various Wulff shapes $\mathcal{W}_\gamma$, and for various initial shapes. We identified the conditions for which stepping will occur by stability and variational arguments; proof that these are the proper conditions will be published in the mathematics literature. The computational algorithm handles both stepping and merging correctly.

Topological changes do occur in the examples and are readily made. Topological changes generally occur when surfaces contact: In crystalline problems with the restriction that, if $\mathbf{n}$ is in $\mathcal{W}_\gamma$ so is -$\mathbf{n}$, the contact is along parallel plane segments; sometimes the adjacancy conditions are not preserved, and infinite weighted curvatures occur for the missing facets, but these infinities are easily handled by introducing a fan of orientations at the corners. This restriction on $\mathcal{W}_\gamma$ limits the applicability to crystals with some symmetry; in 2-D, a two-fold or an inversion axis is sufficient, and, in 3-D, intersecting 2-fold axes, 2/m or an inversion center is sufficient, but crystals with lower symmetries could satisfy this condition, since there is no requirement that $\gamma(\mathbf{n}) = \gamma(-\mathbf{n})$ or even that $\Lambda(\mathbf{n}) = \Lambda(-\mathbf{n})$.

Let us compare the results of the calculations for the square and the regular 16-gon. There is an increase in computational difficulties with increasing N, and this provides a practical limit for the magnitude of N. As long as we stay with regular N-gons, we expect the calculations to converge to that of an isotropic limit, but in this case little is known about this isotropic limit. There are numerical results for the axisymmetric flow in 3D by Nichols and Mullins[12]. Proof of convergence to isotropic flow ($v = \nabla_s^2 H$, where H denotes mean curvature) as the number of sides in $\mathcal{W}_\gamma$ increases is still an open question, but computer experimental evidence indicates that it does.

Although we used a regular 16-gon for $\mathcal{W}_\gamma$, we could just well have taken any irregular convex N-gon, with parallel sides and with N small enough to make calculation feasible, to approximate many anisotropies with low symmetries or combined forms of high symmetry crystals. For example, a combined form with square symmetry with four faces each of direction (10) and (11) would be represented by an octagon often described as a truncated square. If we add eight facets from some (hk), $\mathcal{W}_\gamma$ is a 16-gon that can be used to approximate the anisotropy of many crystals whose lattices have the symmetry of a square.

The comparison of SD vs. SALK shows a number of salient phenomenae which will be discussed below; they are:

- There is a proximity effect which occurs in SD but not in SALK which readily distinguishes the two transport mechanisms by observation.
- Topological changes are possible for both SD and SALK. With identical $\mathcal{W}_\gamma$ and initial shapes, under some conditions they occur in both; sometimes they occur in one but not the other. Although we feel they are more likely to occur in SD than in SALK, we have displayed an example where it occurs in SALK but not in SD.
- A closed surface in which all of the nonzero curvature facets have the same sign of κ^γ can develop facets which have the opposite sign during SD but not during SALK.

Let us discuss these in more detail, beginning with proximity and stepping effects. When the initial shapes are long rectangles steps form immediately in SD and growing bulbs form at the ends of the rectangles. The growth of the bulbs has the effect of diminishing local gradients of the chemical potential and drives the system to look locally like the underlying $\mathcal{W}_\gamma$. The local removal of gradients produces the proximity effect. In SALK, the stepping does not occur; if incipient bulbs are placed in the initial data by forcing non-zero lengths steps onto the long sides, they disappear on a short time scale. These calculations suggest that, because of the proximity effect, it should be possible to distinguish between the two extreme types of area-conserving flow by observing how shapes evolve. We feel that such reasoning from qualitative shape changes is a simpler and more reliable hallmark of mechanism than methods based on scaling laws applied to some set of stereological measures, in which values are plotted on a log-log plot and exponents are used to determine which is the active diffusive mechanism in some materials process. Such averaging is open to misinterpretation and conclusions are often equivocal. Of course, there are mixed cases where neither process is dominant and calculations of such cases will be presented elsewhere. However, scaling laws would do no better when no mechanism is dominant: interpolation of scaling exponents is suspect.

The whole motion is very stable, except for near some of the topological changes. The final state is independent of the number of infinitesimal steps if more than required are inserted, and is also insensitive to using ad hoc step positions in the initial data. This is an indication that the stepping algorithm by which a stable potential is obtained effectively finds a unique potential. A theorem about such uniqueness will appear elsewhere [8]. Computer experiments where steps where injected at random onto the surface $S(t)$ at each forward difference iteration and did not produce behavior different from that with implementation of the stepping algorithm alone.

While the breaking into separate particles of the staircase in Figure 5, the the bulb formation in Figures 3-4, and the formations of inclusions in 7 is reminiscent of Rayleigh-like instabilities such as that calculated in 3-D by Nichols and Mullins[12], they are not really related to it at all since this is a two dimensional model. The Rayleigh instability is is based on a path of continuously decreasing surface area in 3-D; the existence of instability is independent of the particular kind of transport mechanism, although the wavelength depends on it. It does not occur in isotropic two dimensional rods. Rather, the occurance of a Rayleigh-like break-up of the long rectangles in our calculations is a combination of the crystallinity and the transport mechanism since it does not occur in Figures 3-4 for SALK and since the staircase in figure 5 will always break into only two pieces independent of the length of stairs. It is currently unknown whether the analogies to the staircase's break of figure 5 for N-gonal $\mathcal{W}_\gamma$ will disappear as N is increased, but it is suspected that it will as long as it is a staircase – i.e., the axis of the staircase is not parallele to a facet.

On an atomic scale in 3D, a facet may contain steps, ledges, and surface vacancies which can move about the surface while it is growing. In the crystalline model, any facet is represented a being mathematically flat; so, interpretation of the results can only be made at scales where the averaging out of defect nature of the surface is sensible. Vicinal surfaces will always contain ledges and in the crystalline model are represented as a combination of many flat surfaces; the size of such surfaces assumed to be large enough so that averaging is again sensible. An extrapolation from an atomistic model to the continuized equations of motions presented in this paper will appear in a subsequent publication.

Experimental observations of cubes of MgO particles ($\mathcal{W}_\gamma$ is a cube) which are just barely overlapping along their edges break into two isolated cubes have been made by Rankin[13]. Experimentally, the breaking occurs if the overlapped region, which is a rectangular strip, is small and does not occur if it is large. While our calculations are only two dimensional, there is similarity of her micrographs to our Fig. 5.

The examples repudiate some common misconceptions about microstructural evolution.

It is sometimes stated that a system evolves so as to reduce its total free energy the fastest possible way with no regard to the actual diffusive mechanisms. The contrast between the two types of diffusion in the Figures contradicts this statement. Actually, both mechanisms each decrease the free energy as quickly as possible: but in different metrics, as discussed in [10].

It is sometimes suggested that the free energies of the end-states will determine the equilibrium end-state; this is contradicted by the case of surface diffusion in Figures 5 and 7, in which the system does *not* have the lowest possible energy for its area. Rather, equilibrium occurs when all gradients are extinguished and there is no means for the system to, for instance, remove the metastable equilibrium hole in Figure 7.

The ambient chemical potential Ω can increase continuously in time for the case of SALK for any set of positive crystals (and decreases for any set of negative crystals). This is apparent from Eqs. 17–the numerator is a constant if all the mobilities are while the denominator can only decrease. Mass would tend to flow from a system of unequilibrated surfaces to a system which contains only Wulff shapes. The average chemical potential can change discontinuously when a topological change occurs such as when a particle disappears. Such considerations apply to the standard isotropic mean-field coarsening models as well.

In this paper we have described two different types of area-preserving motion for completely faceted two-dimensional interfaces and have established rigorous rules for their motion. The crystalline method has now been used to examine four different types of flows: motion by mean curvature [3] and crystal growth in a diffusion field [2] as well as surface diffusion and surface attachment limited kinetics. The calculated results seem to be qualitatively consistent with experimental observations, although three dimensional flow is a topic for future research. Open questions about two-dimensional behavior remain, and will be addressed in a forthcoming publication.

7 Acknowledgements

Our work on this project was greatly facilitated by the support of ARPA, NSF, the Office of Intelligent Processing at NIST, and the use of the facilities and expertise of The Geometry Center. The physical and morale support of the Handwerker Hotel was also much appreciated. The authors also wish to acknowledge helpful conversations with Jim Warren, and Rob Almgren. Thanks also to Richard Braun and Simon Brandon for critical reading of this manuscript.

References

[1] Jean E. Taylor, John W. Cahn, and Carol A. Handwerker. Geometric models of crystal growth (Overview no. 98-1). *Acta Metall. Mater.*, 40:1443–1474, 1992.

[2] Andrew Roosen and Jean Taylor. An algorithm for the computation of crystal growth in a diffusion field using fully facetted interfaces. *J. Comp. Phys*, 1993. In Press.

[3] Jean E. Taylor. Motion by crystalline curvature. In Jean E. Taylor, editor, *Computing Optimal Geometries*, Selected Lectures in Mathematics, pages 63–65. American Mathematical Society, Providence, RI, 1991. Report and video.

[4] Jean E. Taylor. Mean curvature and weighted mean curvature (Overview no. 98-2). *Acta Metall. Mater.*, 40:1475–1485, 1992.

[5] P.M Girao. Convergence of a crystalline algorithm for the motion of a simple closed convex curve by weighted curvature. *SIAM J. Numer. Anal.*, 1994. In press.

[6] P.M. Girao and R.V Kohn. Convergence of a crystalline algorithm for the heat equation in one dimension and for the motion of a grph by weighted curvature. *Numer. Math.*, 67(1):41–70, 1994.

[7] H.M. Soner. Personal Communication.

[8] J.E. Taylor W.C. Carter, A.R. Roosen. Surface diffusion on fully faceted crystals. Unpublished, 1994.

[9] J.W. Cahn J.E. Taylor. Surface motion and gradient flows. *Stat. Phys.*, 1994. In Press.

[10] J.W. Cahn J.E. Taylor. Gradient flows and surface motion. *Acta Met.*, 1994. In Press.

[11] Fritz John. *Lectures on Advanced Numerical Analysis*. Gordon and Breach, New York, 1967.

[12] W.W. Mullins F.A. Nichols. Morphological changes of a surface of revolution due to capillarity-induced surface diffusion. *J. App. Phys.*, 36:1826–1835, 1965.

[13] L.A Boatner J. Rankin. Unstable neck formation during initial stage sintering. *J. Am. Ceram. Soc.*, 1994. In Press.

Figure 1: Meaning of $\sigma(e)$.

Figure 2: Illustration of the elimination of small, fast-moving edges.

Figure 3: Time evolution of an elongated rectangle with a square Wulff shape. Light gray is motion by SD, while dark gray is SALK. Animated versions of the figures are available in an MPEG format via Mosaic[?], giving an excellent illustration of the nature of the flows.

Figure 4: Time evolution of an elongated rectangle with a regular 16-gon Wulff shape. Light gray is motion by SD and dark gray is SALK.

Figure 5: Time evolution from a "staircase" initial condition with a square Wulff shape. Note that the particle splits in SD but not in SALK. Light gray is motion by SD and dark gray is SALK.

Figure 6: Time evolution from a L-shaped initial condition in which the long leg has been made very long. The Wulff shape is a square. Note that the step on the outside of the shorter leg must 'disappear' and then 'reappear' with the opposite sense as the bulb rounds the corner. Light gray is motion by SD and dark gray is SALK.

Figure 7: Time evolution from a complicated spiral with a square Wulff shape. SALK evolution is not shown.

Figure 8: A demonstration that it is possible for topological changes to occur under SALK, even when such changes may not occur for SD. The Wulff shape is a regular octagon. Light gray is motion by SD and dark gray is SALK.

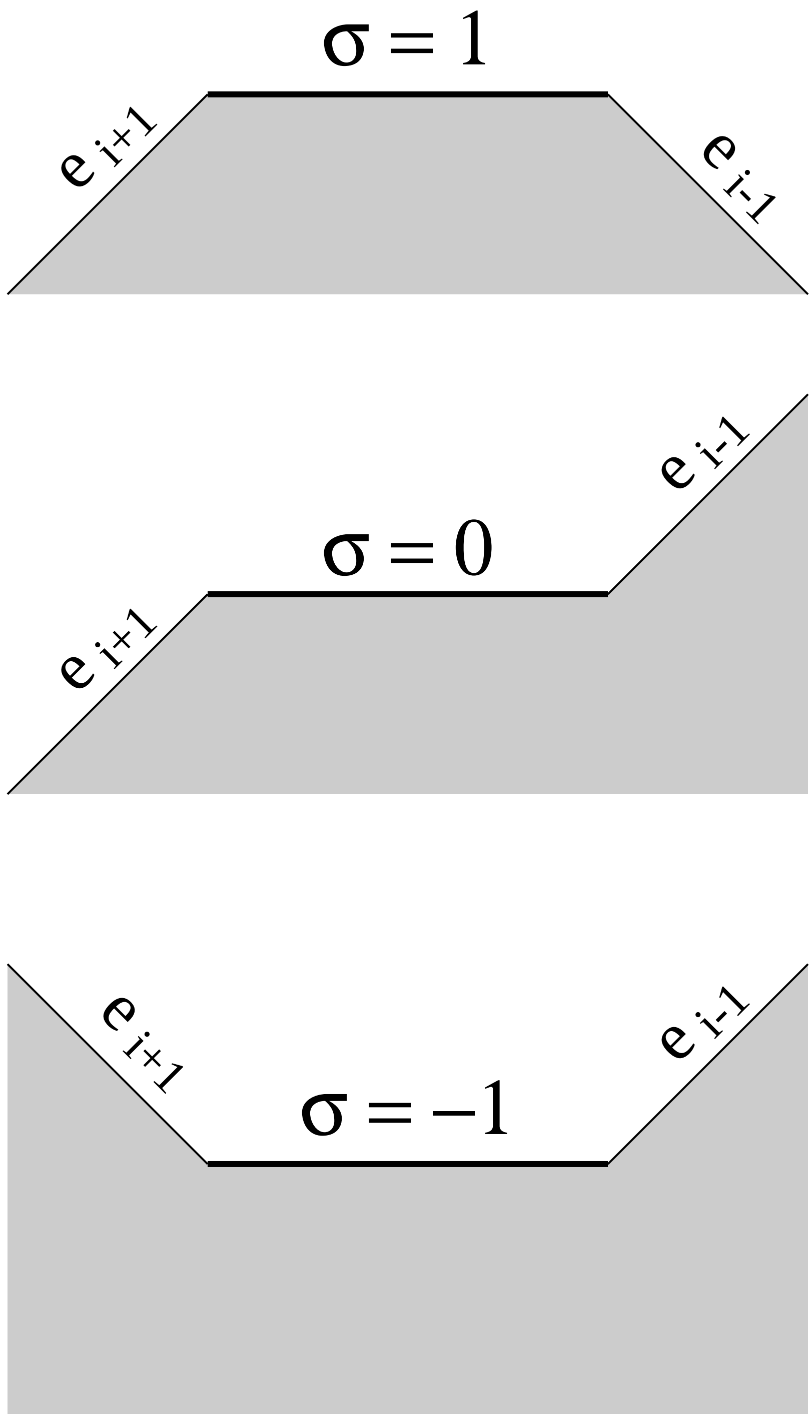
σ = 1
e i+1
e i-1
σ = 0
e i+1
e i-1
σ = −1
e i+1
e i-1

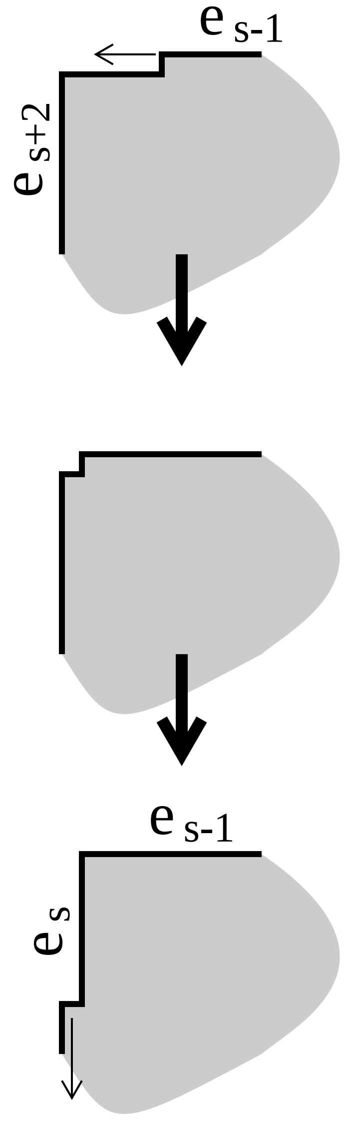

e_{s-1}
e_{s+2}
e_{s-1}
e_s

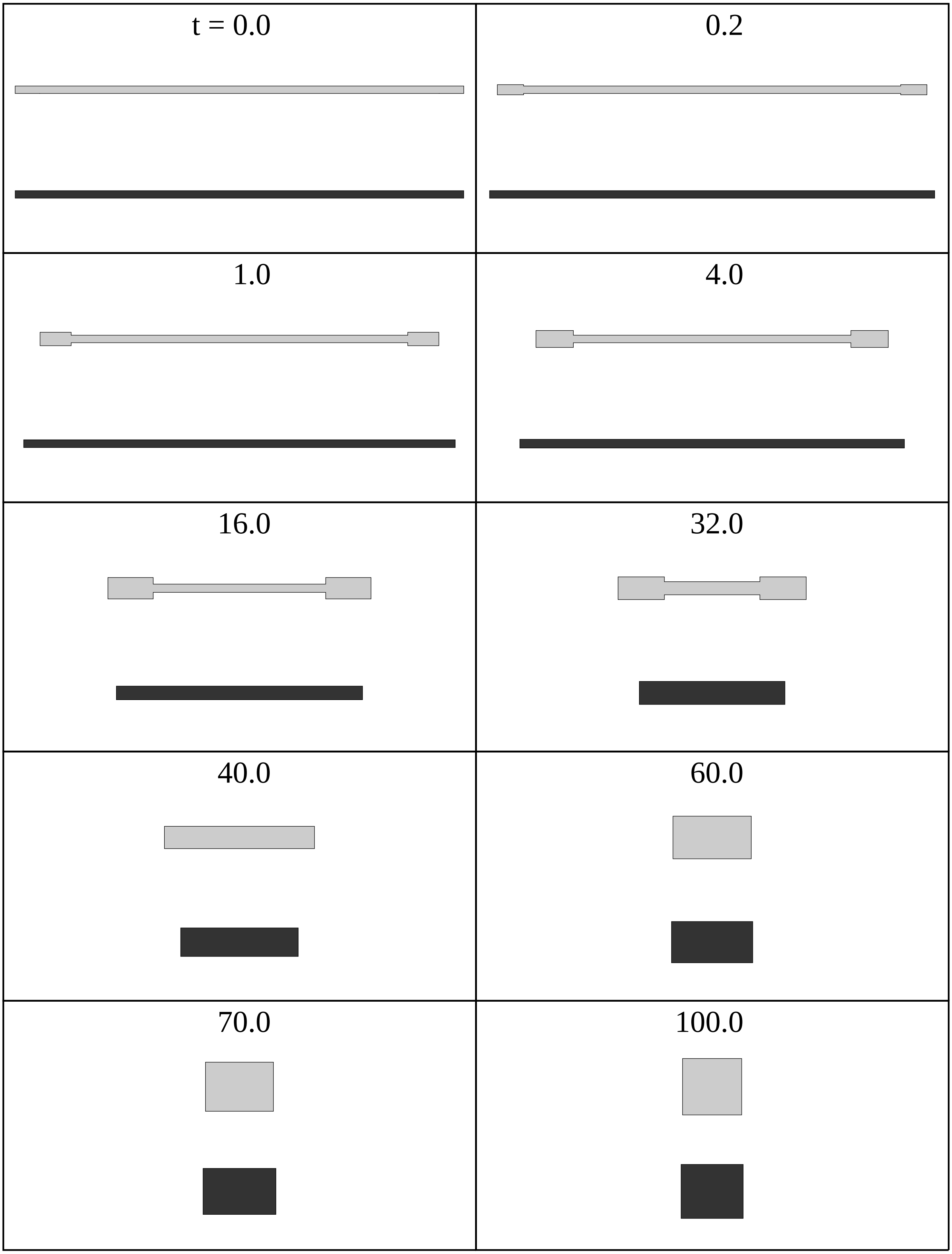
t = 0.0
0.2
1.0
4.0
16.0
32.0
40.0
60.0
70.0
100.0

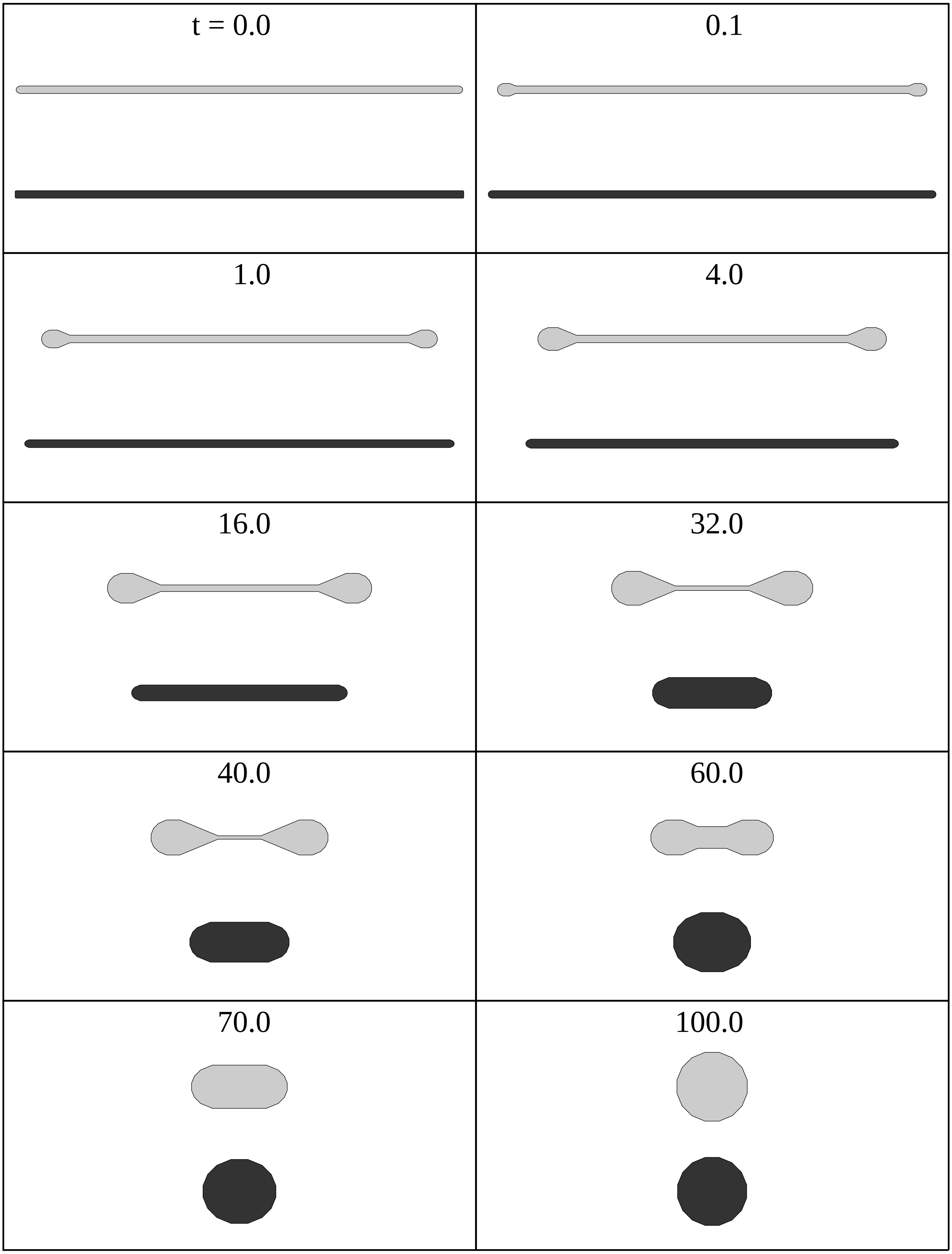

t = 0.0
0.1
1.0
4.0
16.0
32.0
40.0
60.0
70.0
100.0

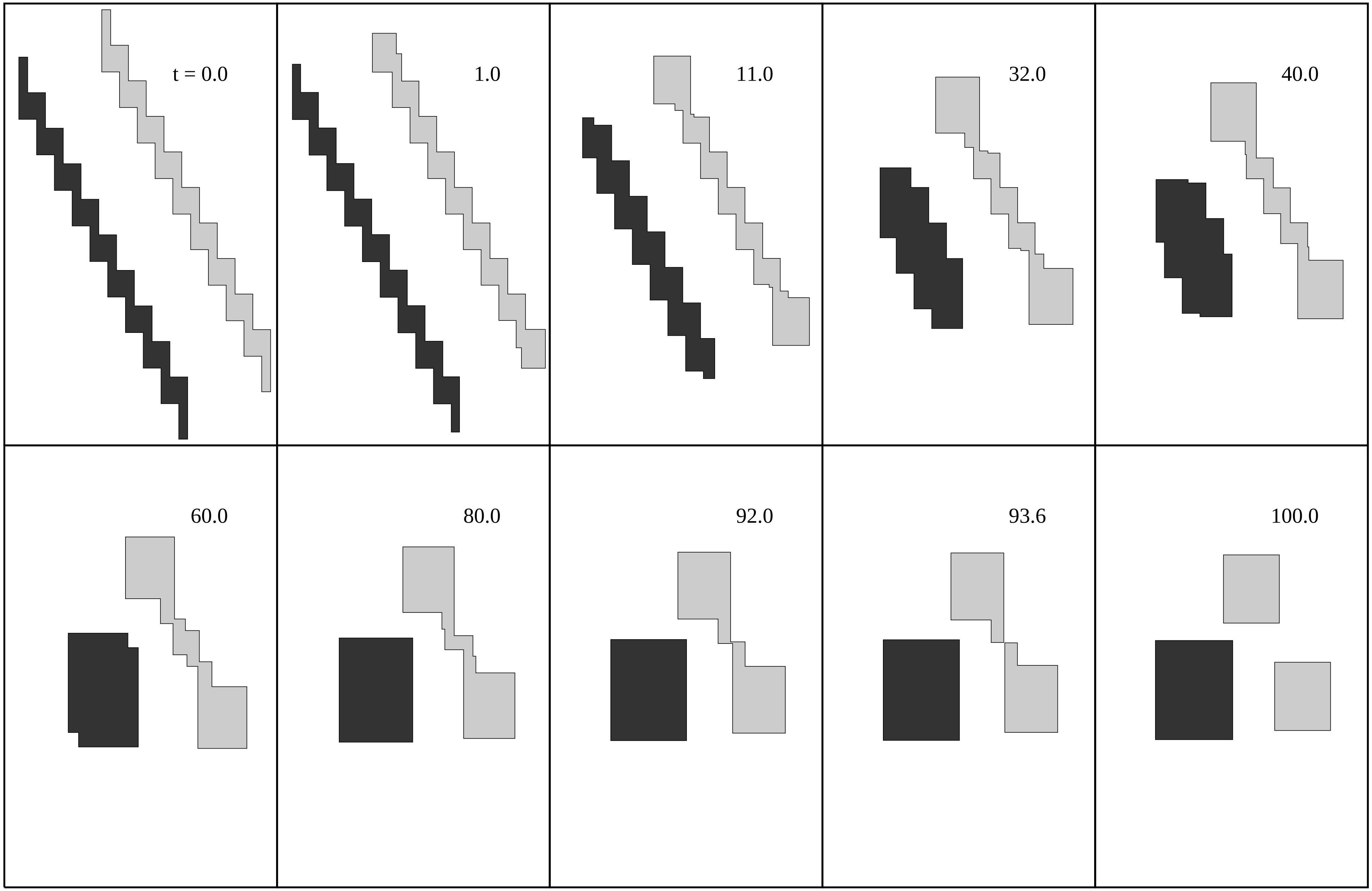
t = 0.0
1.0
11.0
32.0
40.0
60.0
80.0
92.0
93.6
100.0

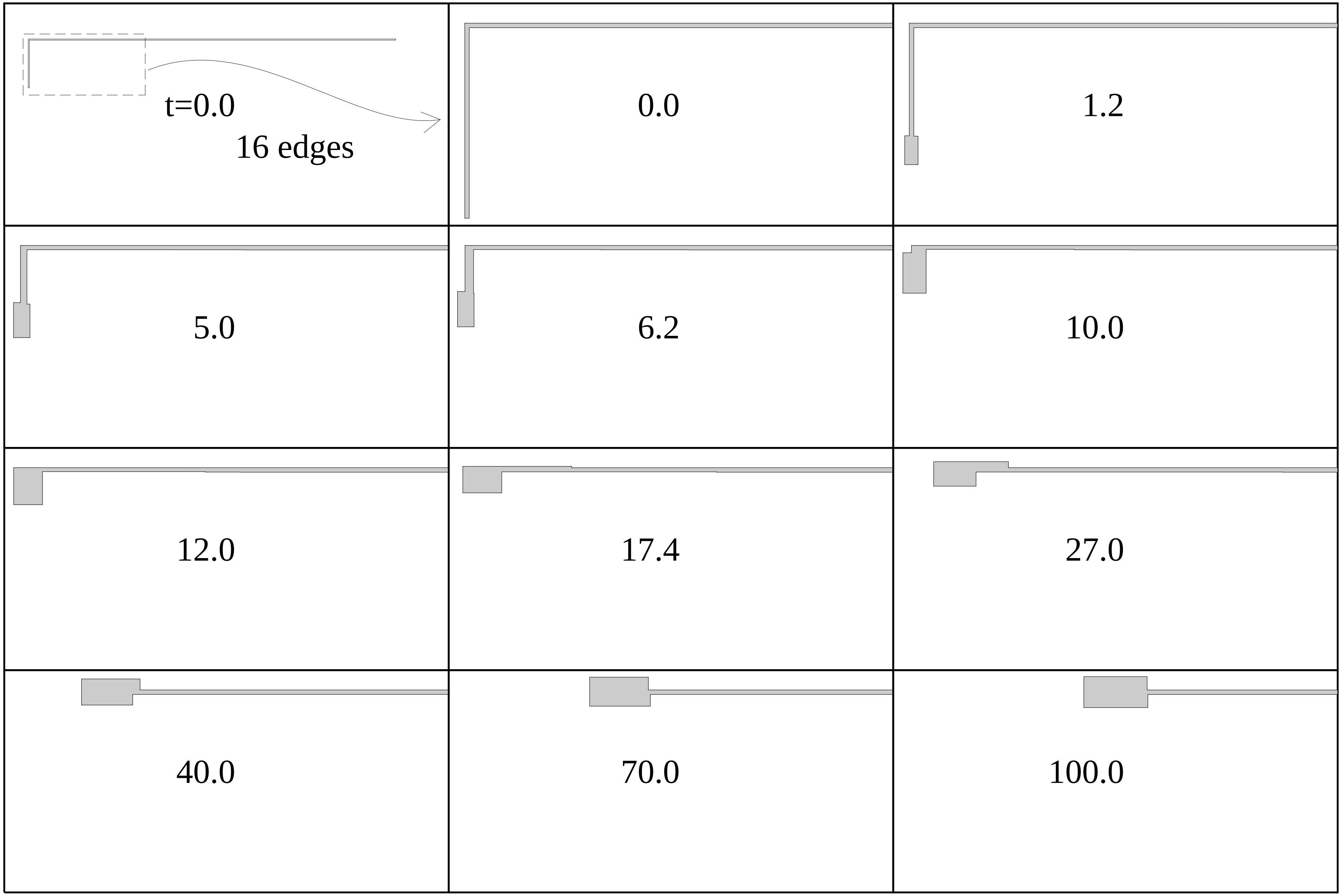

t=0.0
16 edges
0.0
1.2
5.0
6.2
10.0
12.0
17.4
27.0
40.0
70.0
100.0

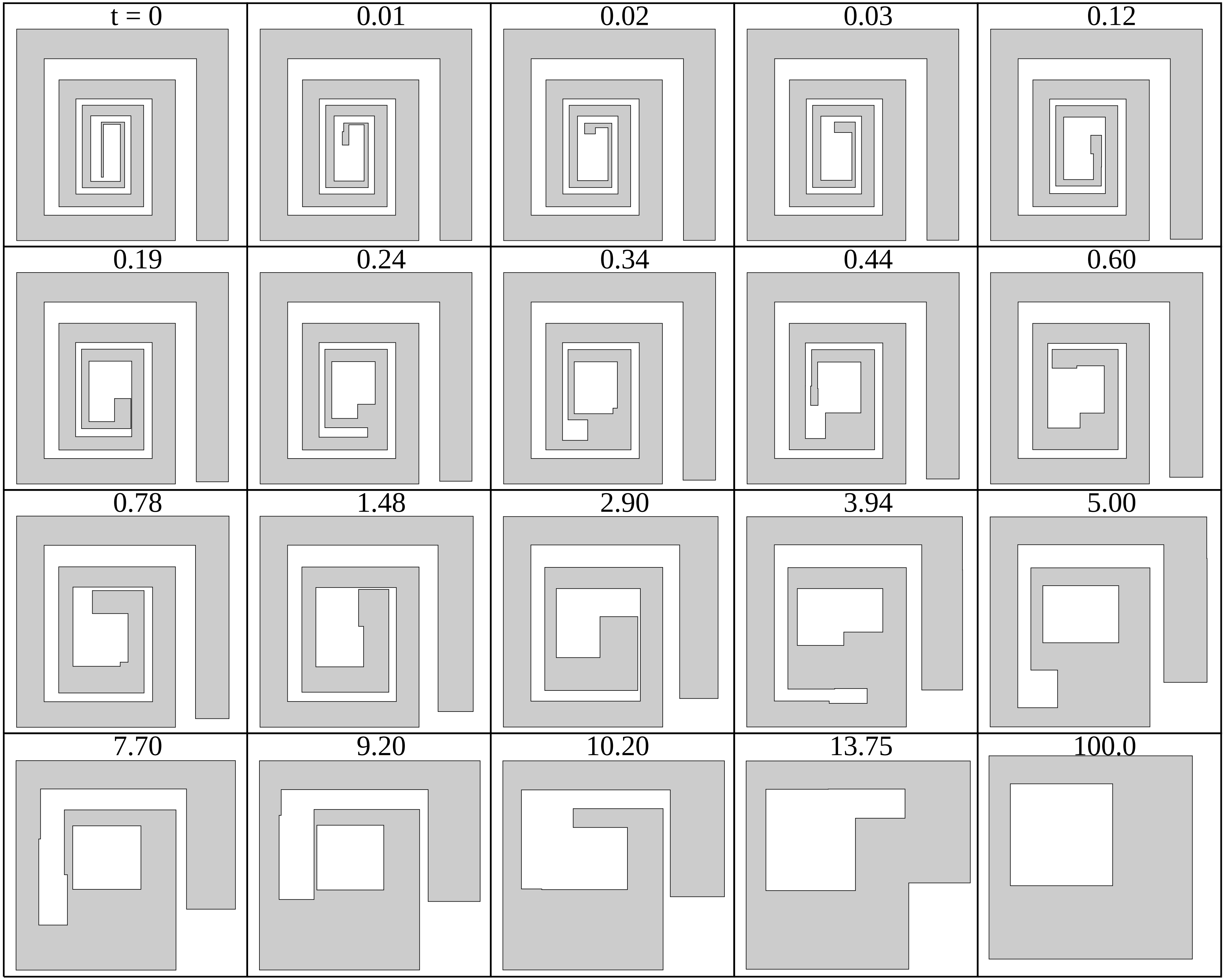
t = 0
0.01
0.02
0.03
0.12
0.19
0.24
0.34
0.44
0.60
0.78
1.48
2.90
3.94
5.00
7.70
9.20
10.20
13.75
100.0

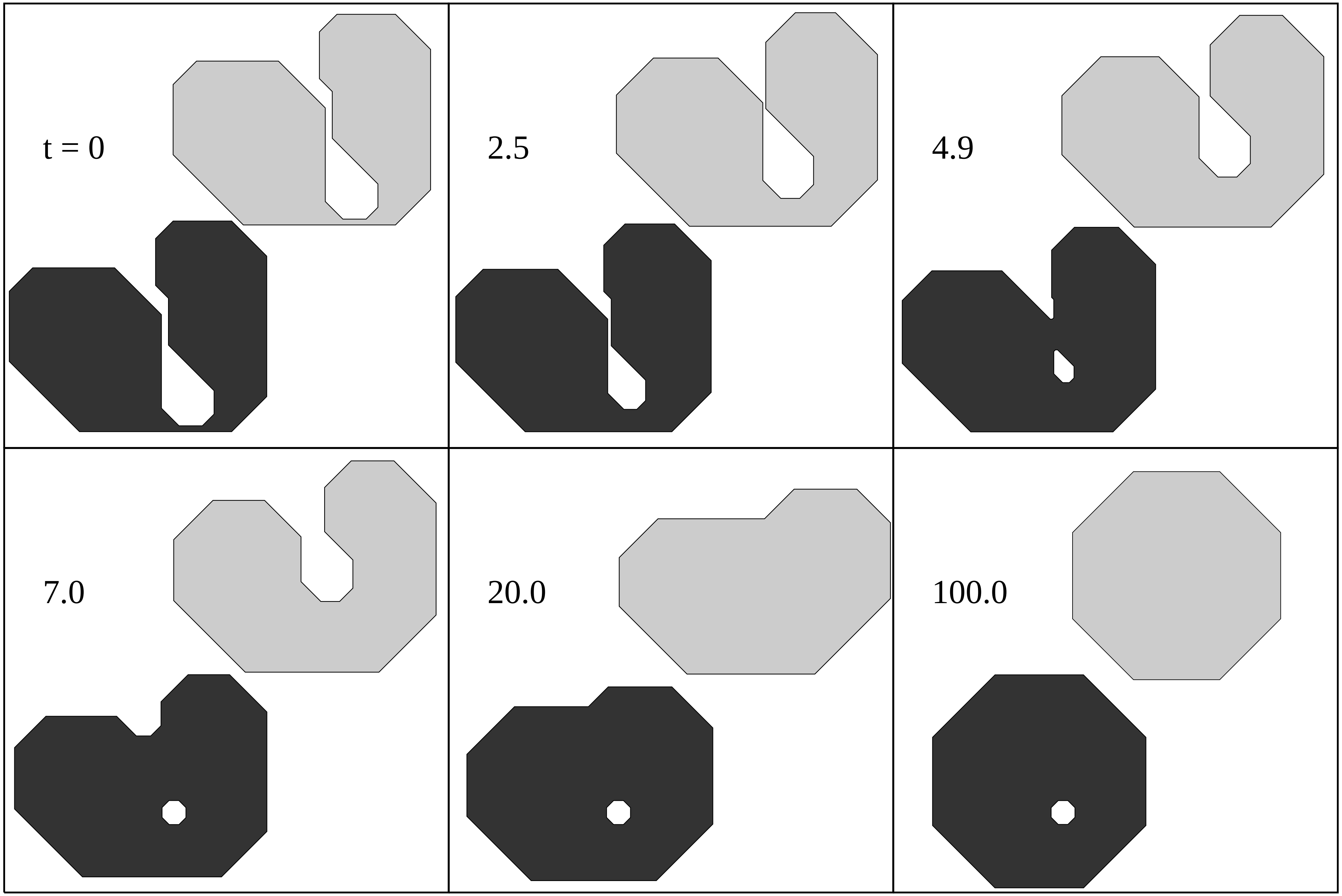
t = 0
2.5
4.9
7.0
20.0
100.0